

# Tethered Lipid Bilayers on Ultraflat Gold Surfaces

Renate Naumann,\* Stefan M. Schiller, Frank Giess, Bernd Grohe,  
Keith B. Hartman,† Iris Kärcher, Ingo Köper, Jörn Lübben,  
Krasimir Vasilev, and Wolfgang Knoll

Max Planck Institute of Polymer Research, Mainz, Germany

Received February 6, 2003. In Final Form: April 3, 2003

Tethered lipid bilayers (tBLMs) were obtained by the fusion of liposomes from diphytanoylphosphatidylcholine (DPhyPC) with self-assembled monolayers (SAMs) of a newly designed archaea analogue thiolipid, 2,3-di-*O*-phytanoyl-*sn*-glycerol-1-tetraethylene glycol-*D,L*- $\alpha$ -lipoic acid ester (DPTL) on template stripped gold (TSG) films from silicon wafer as a template. SAMs, as characterized by reflection absorption infrared spectroscopy (RAIRS), show a mixture of different conformations of the tetraethylene segment in air, which appears to rearrange into the fully extended conformation when the SAM is immersed into an aqueous electrolyte solution, as deduced from thickness measurements by surface plasmon resonance spectroscopy (SPR). The fusion of liposomes was followed by SPR, quartz crystal microbalance (QCM), and fluorescence microscopy. Highly resistive tBLMs were obtained, as demonstrated by electrochemical impedance spectroscopy (EIS) results, which are equivalent to those for the BLM. This large resistivity is attributed to the ultraflat surface of TSG, as well as to the distinctive architecture of the newly designed molecule. The roughness of the TSG obtained from mica and silicon wafer as template was determined by AFM and compared to that of a Au(111) surface on mica. The largest roughness features of TSG are shown to be 0.5–1 nm, which is small compared to the vertical dimension of the DPTL molecules. This is regarded to be crucial for the self-assembly process, particularly in the case of amphiphilic molecules.

## Introduction

Tethered lipid bilayers (tBLMs),<sup>1–5</sup> also referred to as hybrid bilayer membranes (HBMs),<sup>6,7</sup> on planar surfaces constitute an important step toward the biomimesis of the lipid bilayer membrane. They are based on so-called thiolipids<sup>5–12</sup> consisting of a lipid tail and a hydrophilic spacer attached to the solid substrate via a mercapto-linker functionality. Self-assembled monolayers of such molecules form an amphiphilic supramolecular array of a lipid film with a hydrophilic submembrane space, mimicking the cytosol. Due to the covalent attachment of the linker to the surface, the tethered molecules endow the lipid film with a robustness much greater than that of the bilayer lipid membrane (BLM). The planar arrangement, particularly on a metal substrate, allows for the application

of a variety of surface-analytical techniques. The metal surface allows for the investigation of the lipid bilayer under a defined electric field. Hence, tBLMs are useful in basic research, particularly as far as membrane proteins are concerned,<sup>13–18</sup> but also for biosensor applications. Considerable progress has been made in this field.<sup>1–21</sup> Most of the existing model systems, however, suffer from certain drawbacks; in particular, they have insufficient insulating properties. Two causes of the insufficient properties are (i) the architecture of the tethered molecule and (ii) the structure and morphology of the substrate.

Regarding the tethered molecules, some of them make use of alkyl chains,<sup>9,10,16,17,18</sup> phospholipids,<sup>13–15,19</sup> cholesterol,<sup>8,21</sup> or phytanyl groups<sup>4,5,7,11,12</sup> as lipid tails. The phytanyl functionality is a lipid moiety well-known from extremophiles or archaea<sup>22</sup> to form stable membranes under extreme conditions. Considering that the necessary Au surfaces are certainly artificial with respect to their chemical and physical properties (e.g. surface forces), a novel archaea analogue thiolipid has been designed, depicted in Figure 1.

\* To whom correspondence should be addressed. E-mail: naumannr@mpip-mainz.mpg.de.

† Summer student at the MPIP from the Augustana College Sioux Falls, SD.

- (1) Sinner, E. K.; Knoll, W. *Curr. Opin. Chem. Biol.* **2001**, *5*, 705.
- (2) Knoll, W.; Frank, C. W.; Heibel, C.; Naumann, R.; Offenhäuser, A.; Rühle, J.; Schmidt, E. K.; Shen, W. W.; Sinner, A. *Rev. Mol. Biotechnol.* **2000**, *74*, 137.
- (3) Guidelli, R.; Aloisi, G.; Becucci, L.; Dolfi, A.; Moncelli, M. R.; Buoinsegni, F. T. *J. Electroanal. Chem.* **2001**, *504*, 1.
- (4) Raguse, B.; Braach-Maksvytis, V.; Cornell, B. A.; King, L. G.; Osman, P. D. J.; Pace, R. J.; Wieczorek, L. *Langmuir* **1998**, *14*, 648–659.
- (5) Woodhouse, G. E.; King, L. G.; Wieczorek, L.; Cornell, B. A. *Faraday Discuss.* **1998**, *111*, 247–258.
- (6) Vanderah, D. J.; Meuse, C. W.; Silin, V.; Plant, A. L. *Langmuir* **1998**, *14*, 6916–6923.
- (7) Vanderah, D. J.; Pham, C. P.; Springer, S. K.; Silin, V.; Meuse, C. W. *Langmuir* **2000**, *16*, 6527–6532.
- (8) Lang, H.; Duschl, C.; Vogel, H. *Langmuir* **1994**, *10*, 197.
- (9) Cornell, B. A.; Braach-Maksvytis, V. L. B.; King, L. G.; Osman, P. D.; Raguse, J.; Wieczorek, L.; Pace, R. J. *Nature* **1997**, *387*, 580.
- (10) Williams, L. M.; Evans, S. D.; Flynn, T. M.; Marsh, A.; Knowles, P. F.; Bushby, R. J.; Boden, N. *Langmuir* **1997**, *13*, 751.
- (11) Cornell, B. A.; Krishna, G.; Osman, P. D.; Pace, R. J.; Wieczorek, L. *Biochem. Soc. Trans.* **2001**, *29*, 613–617.
- (12) Krishna, G.; Schulte, J.; Cornell, B. A.; Pace, R.; Wieczorek, L.; Osman, P. D.; *Langmuir* **2001**, *17*, 4858.

- (13) Naumann, R.; Schmidt, E. K.; Jonczyk, A.; Fendler, K.; Kadenbach, B.; Liebermann, T.; Offenhäuser, A.; Knoll, W. *Biosens. Bioelectron.* **1999**, *14*, 651–662.
- (14) Schmidt, E. K.; Liebermann, T.; Kreiter, M.; Jonczyk, A.; Naumann, R.; Offenhäuser, A.; Neumann, E.; Kukol, A.; Maelicke, A.; Knoll, W. *Biosens. Bioelectron.* **1998**, *13*, 585.
- (15) Naumann, R.; Baumgart, T.; Gräber, P.; Jonczyk, A.; Offenhäuser, A.; Knoll, W. *Biosens. Bioelectron.* **2002**, *17*, 25–34.
- (16) Krueger, S.; Meuse, C. W.; Majkrzak, C. F.; Dura, J. A.; Berk, N. F.; Tarek, M.; Plant, A. L. *Langmuir* **2001**, *17*, 511–521.
- (17) Glazier, S. A.; Vanderah, D. J.; Plant, A. L.; Bayley, H.; Valincius, G.; Kasianovic, J. J. *Langmuir* **2000**, *16*, 10428–10435.
- (18) Madhusudhana, N.; Silin, V.; Ridge, K. D.; Woodward, J. T.; Plant, A. L. *Anal. Biochem.* **2002**, *307*, 117–130.
- (19) Peggion, C.; Formaggio, F.; Toniolo, C.; Becucci, L.; Moncelli, M. R.; Guidelli, R. *Langmuir* **2001**, *17*, 6585.
- (20) Krysin, P.; Zebrowska, A.; Michota, A.; Bukowska, J.; Becucci, L.; Moncelli, M. R. *Langmuir* **2001**, *17*, 3852–3857.
- (21) Becucci, L.; Guidelli, R.; Liu, Q.; Bushby, R. J.; Evans, S. D. *J. Phys. Chem. B* **2002**, *106* (40), 10410–10416.
- (22) Woese, C. R.; Fox, G. E. *Proc. Natl. Acad. Sci. U.S.A.* **1977**, *74*, 5088.

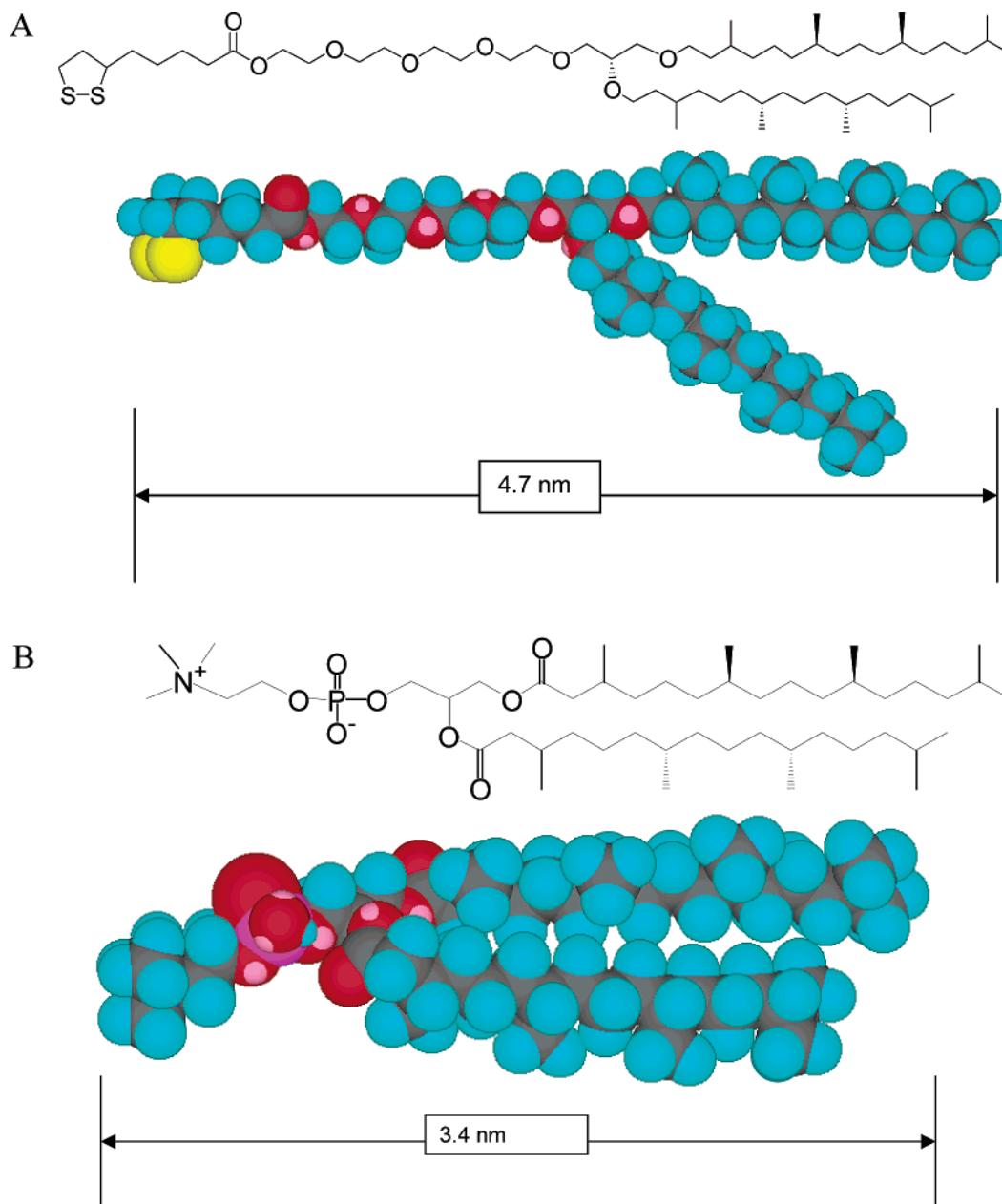


**Figure 1.** Structure and conformation of molecules used for the formation of tBLMs: (A) 2,3-di-*O*-phytanil-*sn*-glycerol-1-tetraethylene glycol-DL- $\alpha$ -lipoic acid ester (DPTL) used to form SAMs; (B) diphytanoylphosphatidylcholine (DPhyPC) used to prepare liposomes which were fused with SAMs. Conformations were obtained by molecular modeling using the program CS Chem 3D Pro.

The lipid moiety should be flexible enough to make up for defects and other irregularities as well as be effectively decoupled from the surface by an appropriate spacer able to accommodate an aqueous phase. The spacer groups used so far were oligoethyleneoxide (OEO) groups<sup>4–12</sup> in most cases, but also peptides.<sup>13–15,19,21</sup> Polymers as spacers are not considered here. With respect to the morphology of the substrate, template stripped gold was studied to consider the significance of the roughness of gold films for the formation of self-assembled monolayers (SAMs). Tethered lipid bilayers have been prepared from the newly designed thiolipid having electrical properties comparable to those of the BLM.<sup>23</sup> A brief outline of the synthesis of the thiolipid, as well as the preparation of the tBLM, has been described in a previous short communication.<sup>24</sup> The

application of the tBLM for the investigation of membrane processes has been demonstrated in the case of valinomycin mediated K<sup>+</sup> transport.<sup>25</sup> More details of the synthesis and the characterization of the thiolipid will be described in a separate paper. Details of the preparation of the tBLMs and their physical characterization are included.

### Experimental Section

The synthesis of 2,3-di-*O*-phytanil-*sn*-glycerol-1-tetraethylene glycol-DL- $\alpha$ -lipoic acid ester lipid (DPTL) was carried out as previously described.<sup>24</sup>

Diphytanoylphosphatidylcholine (DPhyPC) was supplied from Avanti Polar Lipids, Inc., Alabaster, AL; *N*-(7-nitrobenz-2-oxa-1,3-diazol-4-yl)-1,2-dihexadecanoyl-*sn*-glycero-3-phosphoethanolamine, triethylammonium salt (NBD-PE) was from Molecular Probes, Eugene, OR; and ethanol (chromatography grade),

(23) Wiegand, G.; Arribas-Layton, N.; Hillebrand, H.; Sackmann, E.; Wagner, P. *J. Phys. Chem. B* **2002**, *106*, 4245.

(24) Schiller, S. M.; Naumann, R.; Lovejoy, K.; Kunz, H.; Knoll, W. *Angew. Chem., Int. Ed.* **2003**, *42* (2), 208–211.

(25) Naumann, R.; Walz, D.; Schiller, S. M.; Knoll, W. *J. Electroanal. Chem.*, in press.

sodium chloride (SigmaUltra), and potassium chloride were obtained from Sigma-Aldrich. Silicon wafers were purchased from Fraunhofer IIS Bauelemententechnologie, Erlangen, Germany. LaSFN9 high refractive index glass was obtained from Hellma Optik GmbH, Jena, Germany. The two component epoxy glue for optical purposes (EPO-TEK 353ND-4 and EPO-TEK 377) was purchased from Polytec GmbH, Waldbronn, Germany. EPO-TEK 353ND-4 was used for the silicon wafers, and EPO-TEK 377, for the mica sheets.

**Preparation of the Template Stripped Gold (TSG) Surface.** Gold films (50 nm thick) were deposited by electrothermal evaporation (rate 0.01–0.05 nm/s,  $2 \times 10^{-6}$  mbar) on freshly cleaved mica sheets or on silicon wafers. In the case of mica, the gold surface was annealed by heating the mica sheets at 650 °C for 45 s to form Au(111). The gold surface was then glued with EPO-TEK 377 to LaSFN9 high refractive index ( $n = 1.7$ ) glass and cured for 60 min at 150 °C. After cooling, the slides were detached from the mica sheets to expose the TSG film, which was then directly immersed in the thiolipid solution (described in the next section). Gold films on silicon wafers were glued with EPO-TEK 353ND-4, ( $n = 1.5922$ ) to LaSFN9 glass slides and cured for 60 min at 150 °C. Further treatment was the same as that for mica-based TSG.

**Formation of Self-Assembled Monolayers and Vesicle Fusion.** TSG slides were placed for 24 h in an ethanolic solution of 0.2 mg/mL DPTL, rinsed in pure ethanol, and dried in a stream of nitrogen. (The thickness of the SAM was followed by SPR for at least 15 h in a solution of 0.1 mol/L NaCl.) Afterward, liposomes, prepared from DPhyPC by extrusion through 50 nm polycarbonate filters, were added to the solution. Fusion of vesicles was carried out at 30 °C at a final concentration of 0.02 mg/mL. EIS spectra were recorded also in a solution of NaCl 0.1 mol/L.

**Surface Plasmon Resonance Spectroscopy (SPR) and Electrochemical Impedance Spectroscopy (EIS).** The setup to perform these two techniques simultaneously on one sample has been described before.<sup>26</sup> Surface plasmons were excited by a 632.8 nm He/Ne laser. EIS measurements were conducted using an EG&G potentiostat (model 273) and a FRA analyzer (model 1260, Solartron). Spectra were recorded over a frequency range of 1 MHz–5 mHz with an excitation amplitude of 10 mV and a bias potential of 0 V against a Ag|AgCl|NaCl(sat) reference electrode (using a platinum counter electrode). Fitting of spectra to an equivalent circuit was performed with the program ZVIEW (version 2.6, Scribner Associates, Inc.). All measurements were performed at 30 °C.

**FTIR spectroscopy of the DPTL monolayer** was performed on a Nicolet Magna 850 instrument in the reflection absorption mode using a custom-made unit at an angle of incidence of 85° of the p-polarized light. (Measurements were performed with six recordings of 100 scans shuttling between sample and reference while the sample chamber was flushed with dry air.)

**Fluorescence Microscopy.** Liposomes were prepared from DPhyPC mixed with 1 mol % *N*-(7-nitrobenz-2-oxa-1,3-diazol-4-yl)-1,2-dihexadecanoyl-*sn*-glycero-3-phosphoethanolamine, triethylammonium salt (NBD-PE; Molecular Probes, Eugene, OR) by extrusion through 50 nm filters. The extruder was from Milsch equipment, Laudenbach, Germany. Substrates with the lipid monolayers were incubated at 30 °C in suspensions of these liposomes in 0.1 M NaCl solution. Fluorescence was observed as described previously in ref 27 by an inverted optical microscope (Olympus IX-70). The sample was illuminated at a wavelength of  $\lambda = 490$  nm by means of a high-pressure mercury burner (HBO-100) in combination with an interference filter. Emission was detected at  $\lambda = 540$  nm by a light enhancing camera (extended ISIS, Photonic Sciences) and digitized by a frame grabber card (AG-5, Scion, USA).

**Atomic Force Microscopy (AFM) of Gold Surfaces.** AFM images were recorded under ambient conditions on a Nanoscope III microscope (multimode, Digital Instruments) via a 12  $\mu\text{m} \times 12 \mu\text{m}$  scan head and silicon cantilevers (MikroMash). The

cantilevers had a spring constant of approximately 4.5 N·m<sup>-1</sup> and a resonant frequency in the range 135–165 kHz, depending on the spring. The tips of the cantilevers were conical in shape with cone angles of about 20° and radii of tip-curvatures of ~10 nm. The images reported here are raw, unfiltered data obtained by tapping (dynamic) mode at a maximum scan rate of 2 lines s<sup>-1</sup>.

**Quartz Crystal Microbalance Measurements.** The quartz crystal microbalance (QCM) makes use of the change of the resonance frequency of a piezoelectric quartz plate as a function of the thickness of a dielectric layer deposited on its surface. According to the Sauerbrey equation,<sup>28,29</sup> the acoustic thickness,  $d_{\text{ac},f}$  of the layer is proportional to the frequency shift,  $\delta f$ :

$$d_{\text{ac},f} = \frac{m_f}{\rho} = -\frac{\delta f m_q}{f \rho} = -\frac{\delta f Z_q}{f 2f_0 \rho}$$

$m_f$  and  $m_q$  are the mass per unit area of the film and the quartz plate, respectively.  $Z_q$  is the acoustic impedance of the quartz ( $Z_q = 8.8 \times 10^6 \text{ kg} \cdot \text{m}^{-2} \cdot \text{s}^{-1}$ ).  $f$ ,  $f_0$ , and  $\rho$  are the measurement frequency, the fundamental measurement frequency, and the density of the dielectric layer, respectively. Parallel to the resonance frequency change,  $\delta f$ , the change of the half-bandwidth,  $\delta \Gamma$ , of the resonance curve of the quartz is monitored using impedance analysis.<sup>30</sup> By means of a network analyzer (Hewlett-Packard, model 4396A) we measured within a frequency window around the resonance frequency of the QCM. From the plot of conductance versus frequency we obtain the resonance frequency and the half bandwidth at half-height,  $\Gamma$ , by fitting the resonance curve with a Lorentz function. The bandwidth is directly related to the dissipation of the layer,  $D = 2\Gamma/f_0$ . The hardware is controlled by custom-made software<sup>31</sup> and provides a data acquisition speed of about 0.1–1 data sets per second with angstrom resolution. The quartz cell consists of the quartz crystal ( $f_0 = 5$  MHz, polished Au electrodes, Maxtek) placed horizontally in a holder (Maxtek, model CHF200) and allows the recording of measurements on Au surfaces (roughness < 5 nm) in liquid ( $V = 1$  mL) at room temperature. The vesicle solutions were injected into the quartz cell with an Eppendorf pipet ( $V = 50$ – $100 \mu\text{L}$ ).

**Contact angle measurements** were carried out in the advancing angle mode with the fully computer controlled instrument model DSA10-MK2 (Krüss GmbH, Hamburg, Germany), using a drop size of 30  $\mu\text{L}$  and a drop rate of 2  $\mu\text{L} \cdot \text{s}^{-1}$ .

## Results and Discussion

**Novel Archaea Analogue Thiolipid.** 2,3-Di-*O*-phytyl-*sn*-glycerol-1-tetraethylene glycol-D,L- $\alpha$ -lipoic acid ester lipid (DPTL) (Figure 1A) is characterized by two hydrophobic tails, namely the two isoprenoidic phityl chains containing 2,3-di-*O*-diphytyl-*sn*-glycerol, tethered to the substrate via a lipoic acid functionalized tetraethylene glycol spacer. tBLMs were prepared by fusion of liposomes prepared from diphytanoylphosphatidylcholine (DPhyPC) onto SAMs of DPTL, as depicted in Figure 1B. The dimensions of these molecules were obtained by molecular modeling using the program CS Chem 3D Pro with DPTL in an elongated conformation (see this section and further below for the discussion).

The DPTL monolayer was first characterized by RAIRS. The spectrum in air is shown in Figure 2.

The positions of the peaks in the C–H stretching region between 2800 and 3000 cm<sup>-1</sup> (Figure 2A) are typical for the phityl moiety;<sup>32</sup> however, it is complicated by the overlap of C–H stretching vibrations from the oligoethyleneoxide (OEO) segment. Crystalline OEO, for example,

(28) Sauerbrey, G. *Arch. Elektrotech. Übertragung* **1964**, *18*, 617.

(29) Sauerbrey, G. *Z. Phys.* **1959**, *155*, 206–222.

(30) Johannsmann, D.; Mathauer, K.; Wegner, G.; Knoll, W. *Phys. Rev. B* **1992**, *46*, 7808–7815.

(31) Johannsmann, D. *Macromol. Chem. Phys.* **1999**, *200*, 501–516.

(32) Gauger, D. R.; Binder, H.; Vogel, A.; Selle, C.; Pohle, W. *J. Mol. Struct.* **2002**, *614*, 211–220.

(26) Bunjes, N.; Schmidt, E. K.; Jonczyk, A.; Rippmann, F.; Beyer, D.; Ringsdorf, H.; Gräber, P.; Knoll, W.; Naumann, R. *Langmuir* **1997**, *13*, 6188.

(27) Baumgart, T.; Kreiter, M.; Lauer, H.; Naumann, R.; Jung, G.; Jonczyk, A.; Offenhäusser, A.; Knoll, W. *J. Colloid Interface Sci.*, in press.



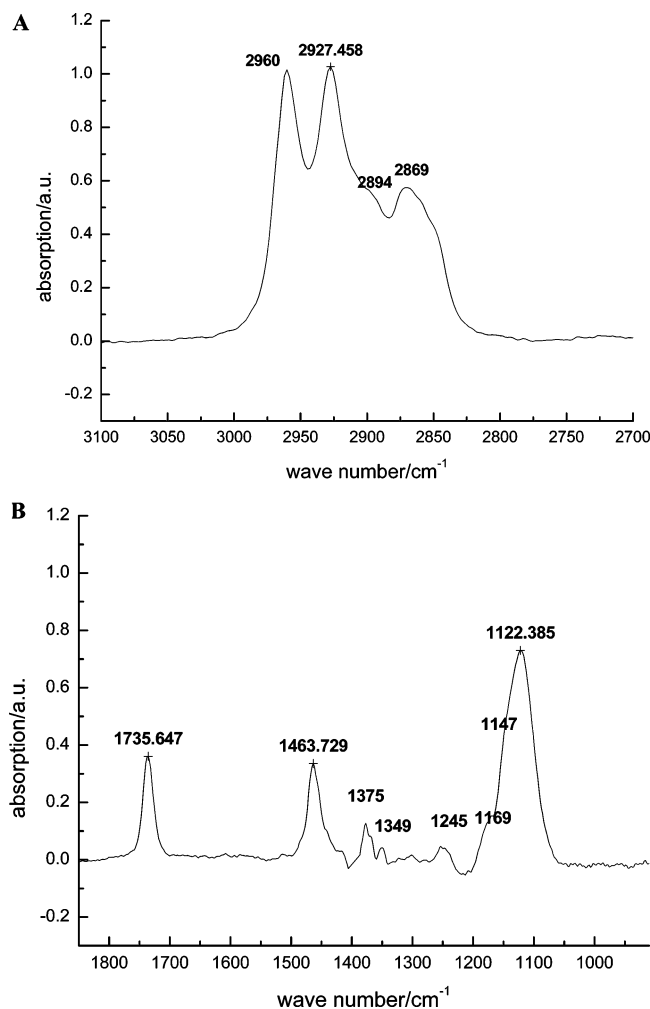


**Figure 2.** RAIRS spectrum in the 2700–3100  $\text{cm}^{-1}$  (A) and 900–1800  $\text{cm}^{-1}$  (B) regions of the SAM of 2,3-di-*O*-phytanyl-*sn*-glycerol-1-tetraethylene glycol-DL- $\alpha$ -lipoic acid ester (DPTL) in dry air, measured with p-polarized light at an angle of incidence of 85°.

is indicated by the shoulder at 2894  $\text{cm}^{-1}$ . The strong band at 1735  $\text{cm}^{-1}$  indicates the carbonyl group of the ester functionality oriented with a portion of the C=O stretch perpendicular to the surface. More information about the conformation of the OEO moiety comes from the region between 950 and 1500  $\text{cm}^{-1}$  (Figure 2B) as compared with RAIRS and IRSE spectra of SAMs obtained from alkylated 1-thiaoligo(ethylene oxides).<sup>6,7</sup> These spectra had revealed a high degree of order of the OEO segment for chain lengths of 5, 6, and 7 with an optimum at 6 EO units.<sup>6,7</sup> Order, in this context, means a 7/2-folded-chain crystal (FCC) helical conformation oriented normal to the surface indicated by bands at 966, 1116, 1243, 1345, and 1460  $\text{cm}^{-1}$ . The octamer, on the other hand, demonstrated a different behavior with a mixture of helical and disordered conformations indicated by a band at 1116  $\text{cm}^{-1}$  and a shoulder at 1130  $\text{cm}^{-1}$ , where disorder means the extended conformation.<sup>7</sup> The OEO segment of the tetramer, decyl thiatetra(ethylene oxide), showed a still higher degree of disorder indicated by a strong band at 1143  $\text{cm}^{-1}$  assigned to the (C–O–C) stretching vibration. Comparatively, the RAIRS spectrum of the DPTL SAM, in the 950 and 1500  $\text{cm}^{-1}$  region, shows features reminiscent of the helical conformation. However, slight inconsistencies can be noted in these spectra, including the absence of the 966  $\text{cm}^{-1}$  band. A strong band does appear at 1122  $\text{cm}^{-1}$  with shoulders at 1147 and 1169  $\text{cm}^{-1}$  as well as a strong band

at 1463  $\text{cm}^{-1}$ . Weak bands are also present around 1245 and 1349  $\text{cm}^{-1}$ . The band at 1122  $\text{cm}^{-1}$  fits perfectly well into the series of spectra of the alkylated 1-thiaoligo(ethylene oxides) starting from the hepta- (1116), hexa- (1118), to the pentamer (1120), which are all predominately considered to be in a helical conformation. A higher ratio of helical to extended conformation as compared to that for the decyl thiatetra(ethylene oxide) could be deduced from the ratio of peak intensities between the 1122 and 1147  $\text{cm}^{-1}$  bands, which can be explained by the differences in the linker functionality. In the case of the alkylated 1-thiaoligo(ethylene oxides), the OEO segment is directly attached to the gold via a thiol group whereas the lipoic acid of the DPTL brings about separation from the gold surface. More flexibility of the OEO segment could also come from the glycerol moiety, but it is more likely to arise from the two phytanyl groups in combination with the all ether functionalities where the diphytanyl moiety represents the hydrophobic part of the molecule instead of only one alkyl group in the case of the alkylated 1-thiaoligo(ethylene oxides). The phase transition temperature of both the 2,3-di-*O*-phytanyl-*sn*-glycerol and the 2,3-di-*O*-phytanyl-*sn*-glycerol-1-tetraethyleneglycol was measured to be –81 °C. Hence, the DPTL SAM should always be in the fluid analogue state so phase separation does not occur, as in the case of alkylated thiolipids,<sup>33</sup> seen from the AFM image (Figure 5D) further below.

**Thickness Measurements by Surface Plasmon Resonance Spectroscopy (SPR).** The simultaneous application of SPR and electrochemical impedance spectroscopy (EIS) to the same sample has proved a very powerful combination in the investigation of tBLMs in the past.<sup>13–15,26,27</sup> Electrothermally evaporated polycrystalline gold films have been used in most cases; see, for example, refs 6, 8, and 9. The roughness of these surfaces, however, can be considerable, amounting to several nanometers in height. We have, therefore, introduced template stripped gold, glued to high refractive index glass by an optical glue which matches the refractive index of the glass substrate.<sup>24</sup> Initially, mica was used as the template due to the relative ease of preparing clean substrates and its superior smoothness.<sup>34</sup> SPR and EIS could be applied simultaneously, as shown in our earlier studies.<sup>24,25</sup> TSG templated from mica suffers certain disadvantages, particularly poor uniformity over large areas, needed for electrochemical studies.<sup>35,36</sup> While detaching the mica from the gold, small fractions of it have a tendency to stick to the gold surface. Therefore, in the present investigation, silicon wafers, covered by a silicon oxide layer, were used as a template which proved to be much more reliable regarding the ease of preparation as well as the reproducibility of the results.<sup>33</sup> Parts A and B of Figure 3 show SPR spectra of TSG with silicon as a template, in air and in 0.1 M NaCl solution, on the bare gold and the monolayer of the thiolipid, before and after fusion of DPhyPC liposomes, respectively.

SPR spectra were simulated using a three layer model including the prism, gold, and thiolipid layers. After vesicle fusion, a fourth layer was added with respect to the phospholipid. The refractive indices used were  $n = 1.7$ ,  $n = 1.84$ ,  $n = 1.45$ , and  $n = 1.52$ , respectively. The thickness of the monolayer in air was always smaller than that in

(33) Stamou, D.; Gourdon, D.; Liley, M.; Burnham, N. A.; Kulik, A.; Vogel, H.; Duschl, C. *Langmuir* **1997**, *13*, 2425–2428.

(34) Wagner, P.; Hegner, M.; Güntherodt, H.-J.; Semenza, G. *Langmuir* **1995**, *11*, 3967–3975.

(35) Priest, C. I.; Jacobs, K.; Ralston, J. *Langmuir* **2002**, *18*, 2438–2440.

(36) Samori, P.; Diebel, J.; Löwe, H.; Rabe, J. P. *Langmuir* **1999**, *15*, 2592–2594.

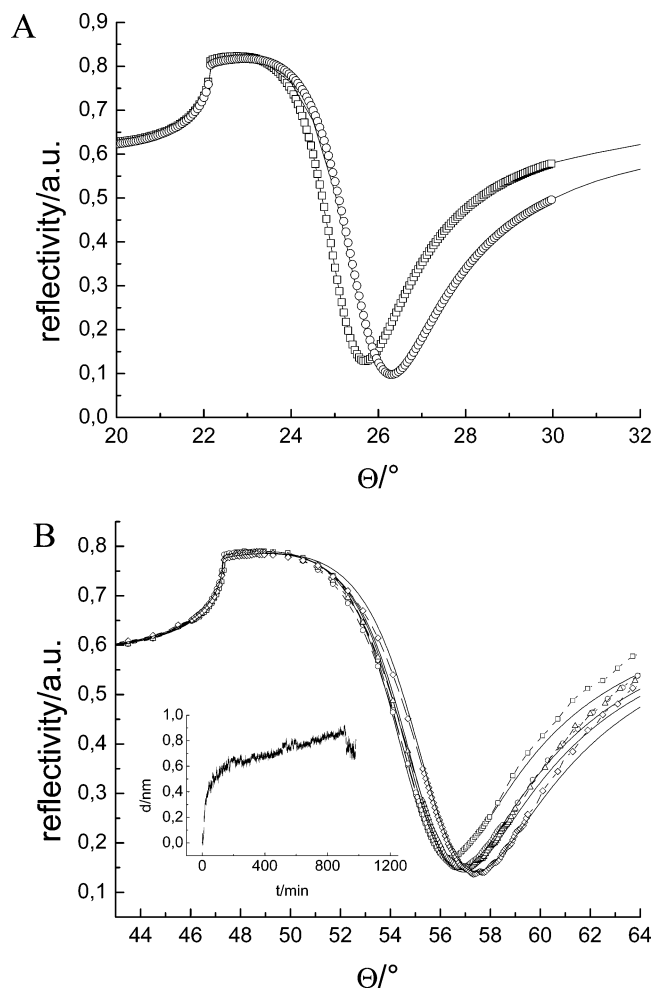


**Figure 3.** Surface plasmon resonance spectra of the bare template stripped gold (TSG) surface (from silicon wafer as template) (squares), in air (A) and in NaCl 0.1 M (B) as well as of TSG coated with a DPTL monolayer before swelling (circles) in air (A) and in NaCl 0.1 M (B), after swelling in NaCl 0.1 M (triangles), and after fusion with DPhyPC liposomes (diamonds). The curves represent simulated spectra using the Fresnel equations<sup>26</sup> for a four-layer system of glass, gold, thiolipid, and phospholipid. Refractive indices of 1.45 and 1.52 were assigned to the thiolipid and the phospholipid, respectively, while the refractive index of the glue was assumed to match that of the glass. The inset shows the change in thickness as a function of time after immersion of the DPTL SAM in 0.1 M NaCl.

the electrolyte, where it increased further as a function of time, as shown in the inset of Figure 3B. Note that the onset of the thickness increase in the electrolyte solution cannot be detected because the recording of the entire spectrum in electrolyte has to be carried out before the kinetic measurement can be started. Thicknesses are compiled in Table 1. The unusually large ranges found, particularly for the thickness of the SAM in air, agree with the same phenomenon found in the case of alkylated 1-thiaoligo(ethylene oxides),<sup>6,7</sup> where they were explained in terms of the different distributions of conformations of the OEO segment in the monolayers, described above.<sup>7</sup> The SAM thicknesses, however, all seem to increase to the same height in electrolyte solution. This is tentatively explained by a relaxation of the entire array of molecules into the extended conformation considering that SPR indicates an increase in the optical thickness or in other words a change in the optical properties of the molecules when the monolayer first comes into contact with electrolyte solution. Short OEO chains were shown by FT-IR studies to undergo unusual conformational changes as a

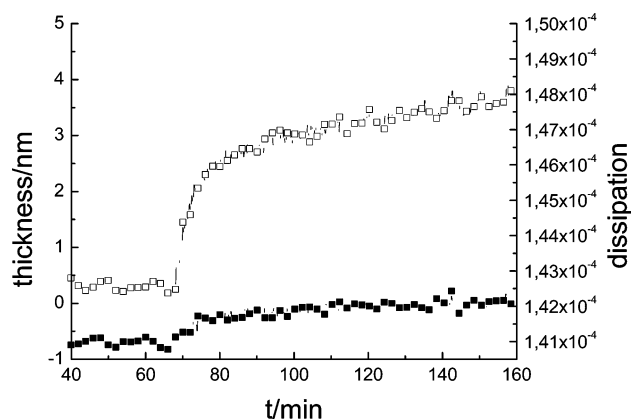


**Figure 4.** Thickness increase according to the change in QCM resonant frequency, assuming a density of 1.2 g/mL, and dissipation versus time during the fusion of liposomes obtained by extrusion of a DPhyPC suspension through a 50 nm polycarbonate filter on a SAM of DPTL in NaCl 0.1 M. The concentration is 0.02 mg of lipid/mL.

function of water uptake, which has been explained in terms of an increase of the dipole moment in the medium with higher dielectric constant.<sup>37</sup> The fast phase of the swelling kinetics of the DPTL monolayer is, therefore, assumed to be due to a conformational change of the OEO segment, particularly since the final thickness of the monolayer compares so well to the dimensions of the molecule according to molecular modeling depicted in Figure 1, to an overall-extended conformation. In our earlier work on valinomycin mediated K<sup>+</sup> transport through a tBLM based on a DPTL SAM, the permeation of salt had been calculated to take 15 h by mathematical modeling of these bioelectrochemical processes using the computer program Spice,<sup>25,38</sup> which agrees well with the second phase of the time course of the swelling process. A further increase in thickness occurs during vesicle fusion, as deduced from the kinetic trace of SPR at a fixed angle of incidence (not shown), indicating the spreading of DPhyPC liposomes to a distal lipid monolayer on top of the proximal lipid monolayer of DPTL molecules to eventually form a tBLM.<sup>24,25</sup> The overall thickness of the tBLM (Table 1) agrees sufficiently well with the dimensions of the molecules, given in Figure 1, taking into account an orientation perpendicular to the surface.

**Fusion of Liposomes Measured by the Quartz Crystal Microbalance (QCM).** More information about the unrolling and spreading of vesicles to form a tBLM can be obtained by measurements with the QCM. They allow for the discrimination between a mere adsorption and the fusion of vesicles, as shown recently by Keller and Kasemo,<sup>39</sup> by following the change in at least two parameters. Frequency change is mainly related to the change in mass, whereas dissipation is related to changes in viscoelastic and rheological properties. Figure 4 shows the respective parameters during fusion of vesicles of DPhyPC on a DPTL monolayer.

The frequency change corresponds to a thickness increase of 3 nm in accordance with SPR data, which does not seem to saturate, however. This could be due to an additional adsorption of unruptured vesicles occasionally indicated by an increase in the capacitance in EIS experiments and also by fluorescence microscopy; see

(37) Matsuura, H.; Sagawa, T. *J. Mol. Liq.* **1995**, 65/66, 313–316.

(38) Walz, D.; Caplan, S. R.; Scriven, D. R. L.; Miculecky, D. C. In *Bioelectrochemistry: Principles and Practice*, Vol. 1; Caplan, S. R., Miller, I. R., Milazzo, G., Eds.; Birkhäuser Verlag: Basel, 1995; Chapter 2.

(39) Keller, C. A.; Kasemo, B. *Biophys. J.* **1998**, 75, 1397–1402.

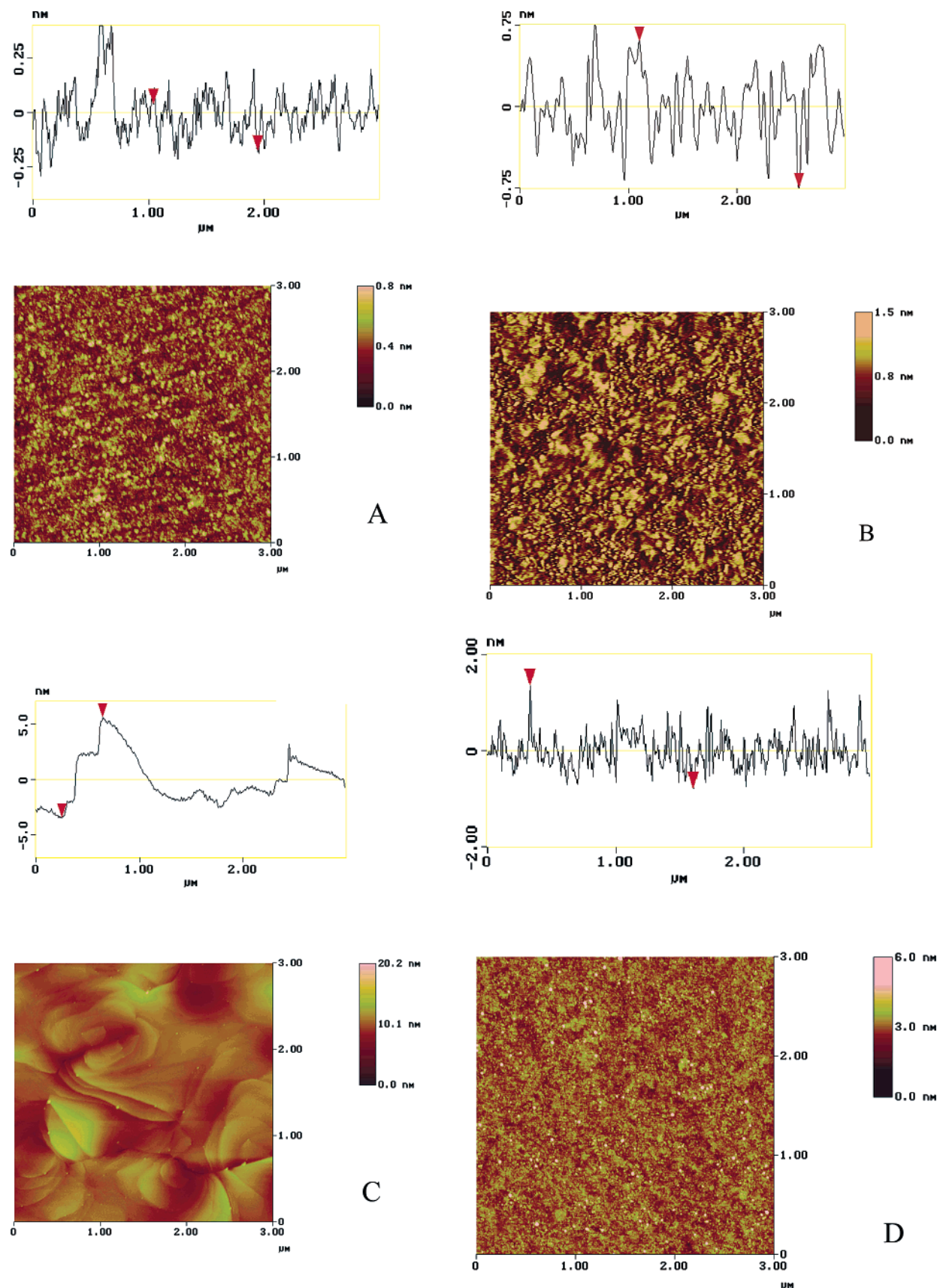


**Figure 5.** AFM images of TSG obtained (A) from freshly cleaved mica and (B) from a silicon wafer covered by an oxide layer used as templates. In part C, Au (111) steps are shown. These were obtained by evaporating gold on freshly cleaved mica and annealing the sample at 650 °C. Part D shows the same sample as part B, covered with a SAM of DPTL. The surface roughness of each sample is given at the top of each part.

further below. The change in frequency is accompanied by only minor changes in the dissipation indicating an

almost complete fusion of the vesicles to form a distal lipid monolayer with the proximal lipid monolayer. The



**Table 1.** EIS ( $C_m$  and  $R_m$  Are the Capacitance and Resistance of the Membrane, Respectively) and SPR ( $d$  = Thickness) Data Obtained by Fitting to the Equivalent Circuit Given in the Inset of Figure 7A and the Fresnel Equations,<sup>26</sup> of the DPTL SAM on TSG Made from Silicon Wafer Template and on Polycrystalline Gold before and after Fusion of DPhyPC Vesicles and after Addition of Valinomycin ( $6 \times 10^{-4}$  M) and KCl (6.89 M)<sup>a</sup>

	$C_m(\text{exp})/\mu\text{F}\cdot\text{cm}^{-2}$	$R_m(\text{exp})/\text{M}\Omega\cdot\text{cm}^2$	$d_{\text{air}}(\text{exp})/\text{nm}$	$d_{\text{NaCl}}(\text{exp})/\text{nm}$ after swelling	$d(\text{calc})/\text{nm}$
DPTL, monolayer on TSG before vesicle spreading	0.71–0.80	3.1–4.9	2.9–3.6	4.5–5.1	4.7
lipid bilayer on TSG after vesicle spreading	0.64–0.72	18–71		8.0–8.5	8.2
lipid bilayer on TSG after vesicle spreading, + valinomycin and 6.89 mM KCl	0.84–1.1	0.0023–0.0026			
DPTL, monolayer on polycrystalline gold before vesicle spreading	0.9	0.029			
lipid bilayer on polycrystalline gold after vesicle spreading	0.9	0.043			
octadecanethiol, monolayer	1.0	13.7	nd	nd	

<sup>a</sup> Ranges of data are from at least three slides. EIS data from octadecanethiol on TSG are added for comparison.

dissipation shift of the thin film, however, is slightly higher ( $1 \times 10^{-6}$ ) than that observed for the formation of a freely floating bilayer on silica ( $0.2 \times 10^{-6}$ ) by Keller et al.<sup>40</sup> This could also indicate additional vesicle adsorption or alternatively swelling of the spacer region. The predominant process, however, seems to be fusion of vesicles, which is in agreement with QCM studies of vesicle fusion on hydrophobic surfaces, for example, on SAMs of alkanethiols.<sup>36</sup> The contact angle of the DPTL monolayer was determined to be  $104^\circ$ , indicating a hydrophobic surface. The role of hydrophobic forces in bilayer adhesion and fusion had been investigated by Israelachvili et al.<sup>41</sup> By contrast, adsorption of vesicles on some hydrophilic surfaces had been shown to cause a substantial increase in the dissipation because of the change in rheological properties due to water entrapment in the vesicles.<sup>39</sup>

**Characterization of the Template Stripped Gold (TSG) Surface.** AFM images of TSG from mica and TSG from silicon wafer, as well as of Au(111), are shown in parts A, B, and C of Figure 5, respectively, together with the roughness analysis. The roughness features of Au(111) over an area of  $1 \times 1 \mu\text{m}^2$  are around 5 nm in height. The roughness decreases by 1 order of magnitude, to 0.5 nm on TSG made from a mica template, as shown in Figure 5A, despite the polycrystalline nature of the Au surface. The roughness features of TSG templated from a Si(111) wafer are about 1 nm in height, as shown in Figure 5B. These features are still low compared to the dimensions of the DPTL molecule under study (Figure 1). Reductive desorption of DPTL monolayers on TSG gave rise to a single reduction peak, illustrated in Figure 6, in accordance with investigations into the reductive desorption of alkanethiols on TSG in which a single desorption peak was also observed.<sup>42</sup>

Reductive desorption of alkanethiols from gold (111), on the other hand, was shown to give rise to double peaks which were attributed to different surface energies of flat terraces compared to the grooves between them. Analysis of the area of the desorption peak of the DPTL SAM resulted in an area of  $51 \text{ \AA}^2$  per molecule, assuming a two electron desorption process assuming both sulfur groups of the lipoic acid moiety bind to the Au surface. This indicates a high packing density considering that the area required by the two phytanyl moieties amounts to  $65 \text{ \AA}^2$ , as calculated by molecular modeling (Figure 1), whereas the area required by the OEO moiety would be much lower. The cross-sectional area of the 7/2 helical OEO segment

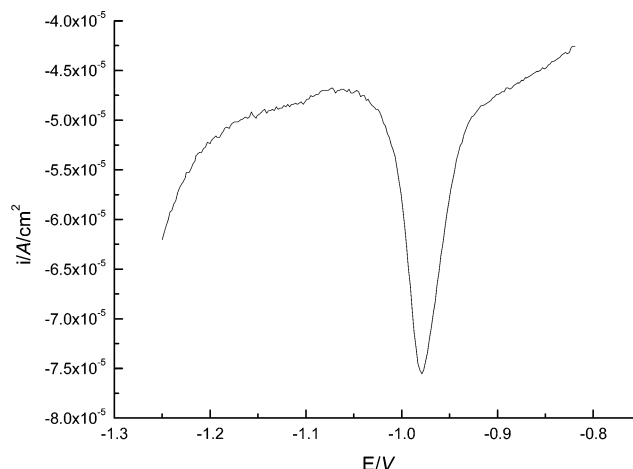


**Figure 6.** Reductive desorption peak of DPTL obtained by cyclic voltammetry of the SAM on TSG from silicon wafer as template in 0.5 M KOH between 0.1 and  $-1.25$  V against a  $\text{Ag}|\text{AgCl}|\text{NaCl}(\text{sat})$  reference electrode, at a scan rate of  $20 \text{ mV/s}$ .

was  $21.38 \text{ \AA}^2$ , as obtained from the X-ray unit cell dimensions of poly(ethylene oxide).<sup>6</sup> Therefore, packing density appears to be dominated by the lipophilic phytanyl tails, even with some interdigitation, whereas the spacer groups in the OEO segment would not be closely packed.

**Electrical Properties of the Lipid Films.** EIS spectra on TSG made from silicon wafer as a template before and after spreading of DPhyPC liposomes are shown in Figure 7A. Electrical parameters, shown in Table 1, were extracted by fitting the data to the equivalent circuit shown in the inset. As compared to the data based on mica as a template shown in our earlier work,<sup>24,25</sup> capacitances of the monolayer and of the bilayer are slightly higher, in accordance with the slightly higher roughness of the TSG. Data obtained from different slides (Table 1) are much more uniformly distributed, in accordance with the more reliable preparation of the TSG. The capacitance and the resistance are fully compatible with the formation of a tethered lipid bilayer starting with a DPTL monolayer, although the capacitance of the tBLM is slightly elevated as compared to the case of a BLM, which is reported to have a capacitance of around  $0.5 \mu\text{F}\cdot\text{cm}^{-2}$ .<sup>23</sup> An example of the respective EIS spectra on polycrystalline gold given in Figure 7B for comparison purposes shows a much lower resistance (Table 1) and a poor reproducibility. A very high resistance was also found in the case of an alkanethiol SAM on TSG (Table 1) also prepared for comparison purposes, not obtainable on

(40) Keller, C. A.; Glasmästar, K.; Zhdanov, V. P.; Kasemo, B. *Phys. Rev. Lett.* **2000**, *84* (23), 5443–6.

(41) Helm, C. A.; Israelachvili, J. N.; McGuigan, P. M. *Biochemistry* **1992**, *31* (6), 1794–1805.

(42) Kakiuchi, T.; Usui, H.; Hobara, D.; Yamamoto, M. *Langmuir* **2002**, *18* (13), 5231–5238.

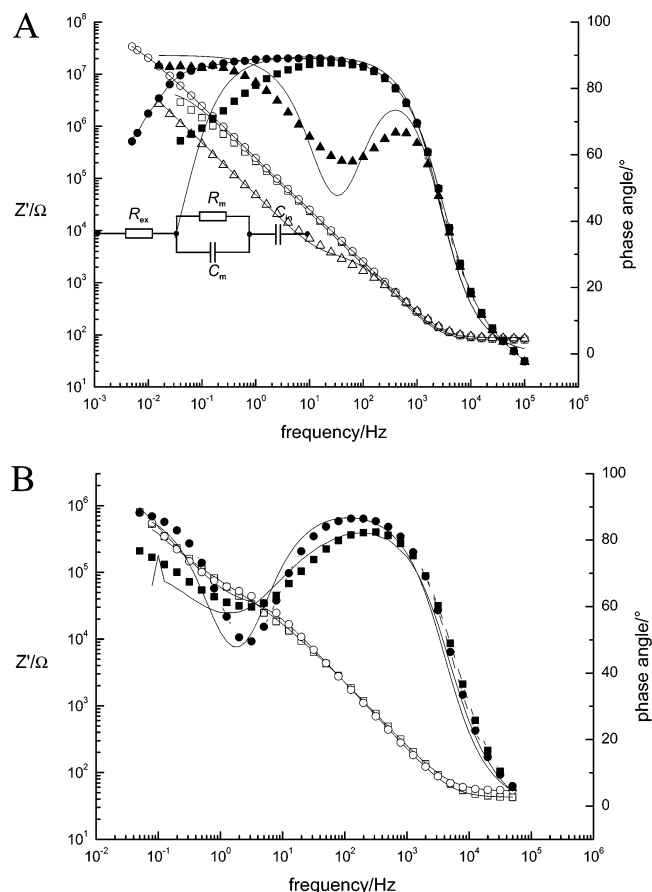


**Figure 7.** Electrical impedance spectra of the DPTL monolayer on a template stripped gold (TSG) surface (from silicon wafer as template) (A) and on polycrystalline gold (B) before (squares) and after vesicle fusion in the absence (circles) and in the presence (triangles) of valinomycin, at  $4 \times 10^{-6}$  M concentration, and 6.89 mM KCl. The magnitude of the impedance,  $Z$ , and the phase angle,  $\theta$ , are represented by open and closed symbols, respectively. Excitation amplitude 10 mV, bias potential 0 against a Ag|AgCl|NaCl(sat) reference electrode. The inset shows the equivalent circuit used for fitting the data.  $R_{ex}$  is the resistance of the bathing electrolyte solution,  $R_m$  and  $C_m$  are the resistance and capacitance of the lipid membrane, respectively, while  $C_{in}$  denotes the capacitance in the spacer region.

polycrystalline gold.<sup>43</sup> The slightly elevated capacitance of the DPTL-based tBLM can be explained in terms of the adsorption of vesicles in addition to the formation of a bilayer, confirmed by fluorescence microscopy (Figure 8).

The fluorescence image of a DPTL SAM after fusion with DPhyPC liposomes (Figure 8) shows a uniform fluorescence with bright spots, which cannot be washed away. The additional adsorption of liposomes, however, does not seem to affect transport processes across the lipid bilayer. This is demonstrated in Figure 7A, where valinomycin mediated  $K^+$  transport<sup>44,45</sup> across the tBLM was observed using TSG made from silicon wafer as a template under conditions identical to those for our earlier reports.<sup>25</sup>

As a first approximation, we adopted the equivalent circuit (Figure 7A) introduced by Cornell et al.,<sup>9</sup> assuming an electrochemical diffuse double layer within the hydrophilic space beneath the lipid film (For the analysis of valinomycin-mediated  $K^+$  transport, see ref 25). This would require the hydration of the OEO spacer region as

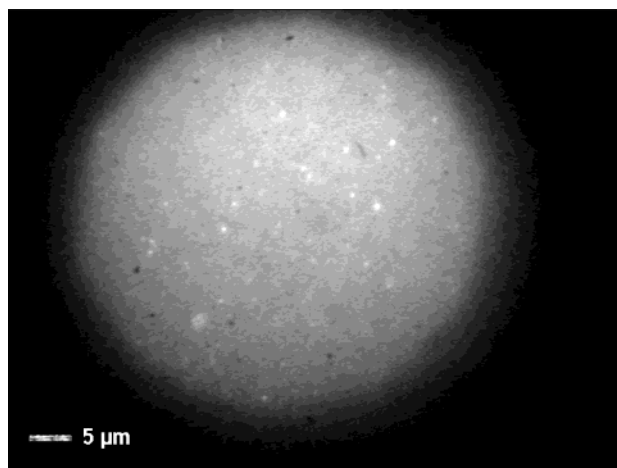


**Figure 8.** Fluorescence microscopy image of the DPTL SAM after fusion with 50 nm liposomes of DPhyPC doped with *N*-(7-nitrobenz-2-oxa-1,3-diazol-4-yl)-1,2-dihexadecanoyl-*sn*-glycero-3-phosphoethanolamine, triethylammonium salt (NBD-PE). The white spots are unruptured vesicles or vesicle aggregates adsorbed to the tBLM.

well as the presence of ions, for example,  $Na^+$ ,  $Cl^-$ , or  $K^+$ , therein. Neutron reflectometry measurements were not conducted on our newly designed thiolipid, DPTL, since a specific instrument is required for such nanometer thin films.<sup>16</sup> As mentioned, in the case of alkylated 1-thiahexa-(ethylene oxide), evidence of an hydrated OEO spacer could not be found.<sup>16</sup> However, the thiahexa(ethylene oxide) has been shown to have an almost perfect ordered  $7/2$  helical conformation, resulting in a very rigid arrangement of the monolayers, which could withstand hydration much better than the less ordered DPTL. Moreover, a strong indication that the OEO segment in the DPTL lipid films could well be hydrated comes from the valinomycin experiment. Carrier-mediated ion transport without a hydrated submembrane space is hardly conceivable. From this, it is assumed that the DPTL lipid films might behave differently from the alkylated 1-thiaoligo(ethylene oxides),<sup>6,7</sup> when the more flexible phytanyl lipid and less tightly packed OEO groups are considered. This could well facilitate the transport of water and ions across the lipid mono- and bilayer, as discussed above in terms of the SPR measurements. DPhyPC films were shown to accumulate water easily.<sup>32</sup>

## Conclusion

In the Introduction, it has been mentioned that some of the tBLMs investigated so far suffer from certain drawbacks, such as insufficient isolating properties,<sup>8,10,13–15,21,23,44</sup> whereas the tBLM, which has properties close to those of the BLM, involves a multicomponent system including a transmembrane lipid to stabilize the membrane.<sup>9,11,12</sup> On account of the newly designed thiolipid, we have been able to prepare tBLMs, on the basis of a single, commercially nonavailable, component, having electrical properties equivalent to those of the bilayer lipid membrane (BLM),<sup>23</sup> but with a more robust tBLM. These tBLMs retained their electrical properties in the fluid cell over a period of days. The effect of the DPTL molecule alone is shown by the QCM measurements, which were impossible to carry out on TSG, because the TSG technique is not easily applicable to the QCM. Measurements indicating the formation of tBLMs were obtained. Moreover, the experiment with the tBLM on polycrystalline gold shows a capacitance compatible with a lipid bilayer, however, exhibiting a considerably lower resistance than

(43) Lingler, S.; Rubinstein, I.; Knoll, W.; Offenhäuser, A. *Langmuir* **1997**, *13*, 7085–7091.

(44) Stark, G.; Ketterer, B.; Benz, R.; Läger, P. *Biophys. J.* **1971**, *11*, 981.

(45) Wagner, M. L.; Tamm, L. K. *Biophys. J.* **2000**, *79*, 1400.



the TSG-based tBLM. This agrees well with the octadecanethiol SAM on TSG (see Table 1) showing an exceptionally high resistance, not found in similar experiments on polycrystalline gold.<sup>42</sup> From this it can be deduced that the smooth gold surface contributes substantially to the good insulating properties of the lipid mono- and bilayers on TSG. Good electrical properties have been obtained from tBLMs on smooth surfaces such as mercury.<sup>19</sup> What has not been observed before, to the best of our knowledge, is the correlation between the roughness effect and the structure and dimension of the molecules. SAMs with perfect supramolecular architecture are obtained only if the vertical dimensions of the molecules are large compared with the roughness of the substrate, while the lateral dimensions allow for the intermolecular interactions to take place without stress. This applies particularly to molecules of higher complexity than, for example, simple alkanethiols. In the case of alkanethiols, intermolecular interactions are still possible due to their overall extended, single hydrophobic domain, which allows a minimum of

hydrophobic interaction, even if they have to arrange on a surface with a roughness of the same order of magnitude as that of the molecules themselves. Considering monolayers of amphiphilic molecules, for example, the DPTL thiolipid, the formation of supramolecular arrays is more complicated. In this particular case, intermolecular forces are clearly dominated by hydrophobic interactions of the double phytanyl tails, requiring more space than the spacer part of the molecule. This results in the very hydrophobic surface of these monolayers in favor of vesicle fusion over adsorption. The spacer, on the other hand, is free to acquire whatever conformation might be convenient to accommodate an aqueous electrolyte layer.

**Acknowledgment.** K.D.H. was supported by the Center on Polymer Interfaces and Macromolecular Assemblies (CPIMA) under NSF-REU Grant #DMR-9820149. LA0342060